MOLECULAR IMAGING AND BIOLOGY

Mol Imaging Biol (2019) 21:1071–1078
DOI: 10.1007/s11307-019-01341-6

Published Online: 8 March 2019

WMIS World Molecular Imaging Society

Check for updates

RESEARCH ARTICLE

In Vitro Assessment of Fluorine Nanoemulsion-Labeled Hyaluronan-Based Hydrogels for Precise Intrathecal Transplantation of Glial-Restricted Precursors

Marcin Piejko,[1,2,3] Piotr Walczak,[1,2,4] Xiaowei Li,[5,6] Jeff W. M. Bulte,[1,2,7,8,9] Miroslaw Janowski[1,2]

[1]*Russell H. Morgan Department of Radiology and Radiological Science, Division of MR Research, The Johns Hopkins University School of Medicine, Baltimore, MD, USA*
[2]*Cellular Imaging Section and Vascular Biology Program, Institute for Cell Engineering, The Johns Hopkins University School of Medicine, Baltimore, MD, USA*
[3]*3rd Department of General Surgery, Jagiellonian University Medical College, Krakow, Poland*
[4]*Department of Neurology and Neurosurgery, University of Warmia and Mazury, Olsztyn, Poland*
[5]*Translational Tissue Engineering Center, The Johns Hopkins University School of Medicine, Baltimore, MD, USA*
[6]*Mary and Dick Holland Regenerative Medicine Program, Department of Neurological Sciences, The University of Nebraska Medical Center, Omaha, NE, USA*
[7]*Department of Biomedical Engineering, The Johns Hopkins University School of Medicine, Baltimore, MD, USA*
[8]*Department of Chemical and Biomolecular Engineering, Whiting School of Engineering, The Johns Hopkins University, Baltimore, MD, USA*
[9]*Department of Oncology, The Johns Hopkins University School of Medicine, Baltimore, MD, USA*

Abstract

Purpose: We studied the feasibility of labeling hydrogel scaffolds with a fluorine nanoemulsion for 19F- magnetic resonance imaging (MRI) to enable non-invasive visualization of their precise placement and potential degradation.

Procedure: Hyaluronan-based hydrogels (activated hyaluronan, HA) with increasing concentrations of fluorine nanoemulsion (V-sense) were prepared to measure the gelation time and oscillatory stress at 1 h and 7 days after the beginning of gelation. All biomechanical measurements were conducted with an ARES 2 rheometer. Diffusion of fluorine from the hydrogel: Three hydrogels in various Vs to HA volumetric ratios (1:50, 1:10, and 1:5) were prepared in duplicate. Hydrogels were incubated at 37 °C. To induce diffusion, three hydrogels were agitated at 1000 rpm. 1H and 19F MRI scans were acquired at 1, 3, 7 days and 2 months after gel preparation on a Bruker Ascend 750 scanner. To quantify fluorine content, scans were analyzed using Voxel Tracker 2.0. Assessment of cell viability *in vitro* and *in vivo:* Luciferase-positive mouse glial-restricted progenitors (GRPs) were embedded in 0:1, 1:50, 1:10, and 1:5 Vs:HA mixtures (final cell concentration $=1 \times 10^7$/ml). For the *in vitro* assay, mixtures were placed in 96-wells plate in triplicate and bioluminescence was measured after 1, 3, 7, 14, 21, and

Correspondence to: Miroslaw Janowski; *e-mail:* mjanows1@jhmi.edu

28 days. For *in vivo* experiments, Vs/HA mixtures containing GRPs were injected subcutaneously in SCID mice and BLI was acquired at 1, 3, 7, and 14 days post-injection.
Results: Mixing of V-sense at increasing ratios of 1:50, 1:10, and 1:5 *v/v* of fluorine/activated hyaluronan (HA) hydrogel gradually elongated the gelation time from 194 s for non-fluorinated controls to 304 s for 1:5 V-sense:HA hydrogels, while their elastic properties slightly decreased. There was no release of V-sense from hydrogels maintained in stationary conditions over 2 months. The addition of V-sense positively affected *in vitro* survival of scaffolded GRPs in a dose-dependent manner.
Conclusions: These results show that hydrogel fluorination does not impair its beneficial properties for scaffolded cells, which may be used to visualize scaffolded GRP transplants with 19F MRI.

Key Words: Hydrogel, Glial-restricted precursors, Fluorine, MRI, Scaffold

Introduction

The field of regenerative medicine currently faces a frustrating paradox: successful and promising outcomes in animal studies, yet failure during clinical trials [1–3]. There is a growing consensus that this discrepancy is driven by anatomical differences between small animals and humans, primarily the difference between the sizes of the central nervous system. The main challenge to successful translation of therapies in the field of regenerative medicine is cell delivery and distribution [4]. Glial-restricted precursors (GRPs) are capable of replacing defective macroglia and have been shown to provide the most beneficial therapeutic effect in small-animal models [5, 6], but only if extensive and global engraftment is achieved [7]. The translation of these benefits to patients with diseases that affect the spinal cord has been challenging [8]. The human spinal cord is much larger than that of a mouse; for widespread cell distribution, multiple intraspinal injections over the entire spinal cord would be required, which is neither safe nor feasible. In addition, access to the spinal cord parenchyma is difficult and requires extensive, complication-prone neurosurgery. The intra-arterial route of cell delivery is highly promising for the treatment of brain disorders due to favorable vascular access [9, 10]. In contrast, the spinal cord is supplied by a network of tiny arteries, which are not easily accessible by endovascular catheters [4]. The intrathecal route, however, is very attractive for cell delivery due to the favorable surface-to-volume ratio of the spinal cord, the minimally invasive character of lumbar puncture, and the facile placement of a catheter [4]. However, cells suspended in solution easily amass after transplantation, losing direct contact with the spinal cord, which may hamper their engraftment. Thus, the embedding of GRPs within a hydrogel might provide the support necessary to keep cells in close proximity to the spinal cord; this would facilitate their readiness for migration into the spinal cord and labeling of a hydrogel may enable precise delivery to the required segment of the spinal cord, as well as report on the process of hydrogel degradation [4].

Among a variety of available biomaterials capable of forming hydrogels, hyaluronan is particularly attractive, as it is a common component of the extracellular matrix [11]. It is a biopolymer of disaccharide (β1,4-D-glucuronic acid and β1,3-N-acetyl-D-glucosamine), which is extracted from tissues or biotechnologically synthesized. It ultimately forms a soluble and viscous liquid. The introduction of easily cross-linkable chemical groups, such as thiols, into hyaluronan monosaccharides opens an attractive possibility of forming hyaluronan-based, three-dimensional hydrogels under physiological conditions [12–14]. Hyaluronan-based hydrogels are considered viable candidates for cellular graft support [15, 16].

There are various approaches to hydrogel imaging, such as radiotracers [17], fluorescent agents [18], traditional magnetic resonance imaging (MRI) contrast agents, such as gadolinium [19], or label-free MRI contrast agents [20], which are tuned to specific experimental needs. The short half-life of radiotracers excludes long-term imaging, and fluorescence is not applicable to invasive destinations like the spinal cord or the intrathecal space. MR imaging of the intrathecal space is also plagued by magnetic field inhomogeneity and susceptibility artifacts, which limit the value of proton-based MR imaging, including the use of superparamagnetic iron oxide (SPIO) nanoparticles. In addition, SPIO-based cell tracking techniques are plagued by difficulties in interpretation, as hypointense signals generated by iron contrast can be confused with hemorrhage, air, and other magnetic susceptibility artifacts. It has also been shown that dying cells release contrast that is internalized by local tissue macrophages and the detected MRI signal cannot distinguish between viable stem cells or phagocytes. 19F MRI is a "hot spot" imaging technique [21] devoid of background signal and the contrast agent removed from dying cells is rapidly cleared from the tissue. 19F hot spot MRI using a clinically applicable fluorine nanoemulsion has already been shown to overcome some of the limitations of using SPIO nanoparticles [22, 23].

The aim of this study was to assess the feasibility of labeling an HA-based hydrogel with a fluorine nanoemulsion to serve as an MRI-visible, injectable scaffold for GRP transplants. This report includes rheological properties, swelling characterization, stability of labeling, and the influence on GRP survival of hydrogels *in vitro* and *in vivo*.

Materials and Methods

Cell Culture

Murine glial-restricted precursors (GRPs) were harvested from second-trimester fetuses, as previously described [12]. Transgenic mice with conditional expression of green fluorescence protein (GFP) under a proteolipid protein promoter (PLP) and the constitutive expression of luciferase were used as donors. GRPs were expanded on polystyrene flasks coated with poly-L-lysine and laminin in the medium consisting of DMEM/F12 supplemented with N2 and B27, bovine serum albumin (BSA), heparin, and β-FGF. The culture medium was exchanged every third day, and, at 70–80 % of confluency, cells were detached by trypsin/EDTA and split 1:3. We used cells at the second to fourth passage for all experiments.

Hydrogel Preparation and Labeling with Fluorine Nanoemulsion

Hydrogels were prepared by the addition of 10 mg/ml of poly (ethylene glycol) diacrylate (PEGDA) dissolved in PBS to 10 mg/ml thiol-modified hyaluronic acid (HA) (HyStem; EsiBio, USA). Labeling of hydrogels was performed through simple mixing of a fluorine nanoemulsion (V-sense, Celsense, USA) with thiol-modified HA at various volumetric ratios of 1:50, 1:10, and 1:5 in a fixed final volume, followed by the addition of a cross-linker at a fixed ratio of 1:4 PEGDA to HA (Table 1). Four hydrogels, including a non-labeled control, were subjected to further investigations.

Rheology

Each freshly prepared hydrogel precursor solution was loaded onto a pre-warmed plate of an ARES 2 rheometer (TA Instruments Inc.). The shear storage (G′) and loss (G″) modulus were measured with a time sweep with the following parameters: temperature = 37 °C; oscillation strain = 1 %; and angular frequency = 6.28 rad/s. Gelation times were designated from the plot of G′ and G″ as a function of time in a place where G′ began to dominate over G″, as described previously [14]. The two series of hydrogels were prepared in 3-mm molds and maintained in a humidified Petri dish at 37 °C to determine their stiffness (G′). The stiffness of hydrogels was examined at 1 h after their gelation and 7 days later, respectively. G′ and G″ were measured using the strain sweep with the same parameters above except for oscillation strain = 1–10 %.

Table 1. Final concentration of Vs, HA, and PEGDA components of the hydrogel

	Concentration in final volume (mg/ml)			Ratio
Hydrogel	Vs	HA	PEGDA	HA/PEGDA
0:1 Vs:HA	0.00	8.00	2.00	4:1
1:50 Vs:HA	5.67	7.87	1.97	4:1
1:10 Vs:HA	26.67	7.41	1.85	4:1
1:5 Vs:HA	49.66	6.90	1.72	4:1

Swelling Measurements

Seven days after gelation, hydrogels were gently purged three times in distilled water, evaporated overnight under a vacuum, and weighed (W_{dry}). Then, hydrogels were immersed in distilled water, agitated at 300 rpm and 37 °C over 24 h. The distilled water supernatant was exchanged six times. After 24 h of incubation, hydrogels were blotted and immediately weighed (W_{wet}). The swelling ratio was calculated as the W_{wet} to W_{dry} ratio.

Stability/Durability Measurements

Each freshly prepared hydrogel was placed in two 10-mm NMR tubes at a final volume of 300 µl, and, once the process of cross-linking was completed, 3 ml of sterile PBS was layered over the hydrogel and maintained at 37 °C throughout the entire experiment. One set of NMR tubes filled with hydrogels was maintained at a static condition, and the second one was agitated at 1000 rpm to additionally challenge the persistence of the fluorine nanoemulsion inside the hydrogel. During the first week, PBS in the tubes was exchanged daily, and thereafter, weekly until the end of the experiment. Four reference tubes containing 0, 3.35×10^{16}, 6.47×10^{16}, and 1.23×10^{17} 19F atoms were used as a reference (Silicone PFC, Celsense, Inc.). The persistence of fluorine labeling was assessed by 19F MRI (Bruker Ascend 750) acquired at 1, 3, 7 days, and 2 months after preparation using a Bruker Ascend 750-Mhz scanner. 19F MRI included a RARE sequence scan with a RARE factor = 8, FA = 90 deg., TE/TR: 5.79/1000 ms, NA = 32, RFA = 180 deg., nuclei reference attenuation: 14 dB, excitation pulse: length = 0.9133 ms, bandwidth = 3000 Hz, scan time: 2 min, 8 s. Hydrogel visualization was first achieved using 1H MRI, and then, was used as a reference for the overlay with 19F images. Voxel Tracker 2.0 (Celsense, Inc.) was used to quantify the fluorine content.

In Vitro Viability of GRPs Embedded within Hydrogels

The viability of GRPs was assessed longitudinally by bioluminescence imaging (BLI). Initially, 100 µl of various mixtures of HA/fluorine nanoemulsion and control HA were placed into a clear-bottomed 96-well white-wall plate (Greiner, USA) followed by the addition of 10 µl of 1×10^7 cells/ml in complete medium to each well. Then, the hydrogels were cross-linked by the addition of 25 µl of

10 mg/ml PEGDA. Ten minutes later, 30 µl of cell culture medium was gently transferred onto the top of the hydrogels, which were then incubated at 37 °C and 5 % CO_2 throughout the experiment. Viability measurements were performed over 28 days using a Victor 3 plate reader (PerkinElmer, USA) after the addition of 70 µl of D-luciferin stock (150 µg/ml) in cell culture medium. Three separate measurements of bioluminescence were acquired with an exposure time of 3 s each. Immediately after imaging, the luciferin solution was replaced with fresh media.

In Vivo Viability of GRPs Embedded Within Hydrogels

The study was approved by our Institutional Animal Care and Use Committee at the Johns Hopkins University. The dorsal side of a rag2$^{-/-}$ mouse was shaved and a day later GRPs were embedded in four different hydrogel formulations being prepared the same way as above for the *in vitro* studies. Two different cell concentrations were used: 1×10^6 and 1×10^7 cells/ml. The mixtures were immediately transferred into 100-µl Hamilton syringes, and before gelation was completed, 20 µl of the cell suspension was injected subcutaneously on the dorsal side of the animal. BLI was performed at 1, 7, 14, and 21 days after implantation using an IVIS Spectrum CT instrument (Perkin Elmer), as previously described.

Results

Rheological Properties

Increasing the concentration of fluorine in the hydrogels resulted in delaying the gelation time: 197, 202, 297, and 304 s for a Vs:HA ratio of 0:1, 1:50, 1:10, and 1:5, respectively (Fig. 1a). Upon macroscopic examination, the addition of higher concentrations of fluorine nanoemulsions (1:50, 1:10, and 1:5 Vs:HA) resulted in a milky appearance and a slightly more fragile structure compared to controls. After extended incubation (at least 24 h after gelation), the milky optical characteristics persisted, but again, appeared fragile when compared to unlabeled gels. These macroscopic observations were consistent with rheology measurements (Fig. 1b). The G′ of unlabeled hydrogels (0:1 Vs:HA) measured at 1 h after the addition of the cross-linker was 183 Pa (100 %). For labeled hydrogels, G′ was 152 Pa (83 % of control) for 1:50, 137 Pa (75 %) for 1:10, and 95.3 Pa (52 %) for 1:5 Vs:HA. After 7 days, G′ was five to six-fold higher than initially, and the difference between controls and fluorine-labeled gels was less expressed: 870 Pa (100 %) for the control hydrogel (0:1 Vs:HA), and 717 (82 %), 732 (84 %), and 588 Pa (68 %) for 1:50, 1:10, and 1:5 Vs: HA hydrogels, respectively.

Swelling Ratio

The swelling ratio refers to the balance of osmotic and elastic forces inside the polymeric hydrogel [24]. We found that the swelling ratio was inversely proportional to the fluorine nanoemulsion content (Fig. 2a) and remained directly proportional to the storage modulus (Fig. 2b). This is in opposition to the theoretical model [24] and other experimental data [14]. We hypothesize that the hydrophobic nanoemulsion retained inside the hydrogel prevents hyaluronan from binding to water and decreases the osmotic forces of whole hydrogels. This would lead to a reduced network density and decreased elasticity.

Stability of Fluorine-Labeled Hydrogels

The concentration of fluorine, as calculated by F-19 MRI signal intensity for non-agitated (1:5, 1:10, and 1:50 Vs:HA 0 rpm) and agitated 1:50 Vs:HA hydrogels, remained high for the first 2 months of incubation (Fig. 3a). Interestingly, 19F signal intensity for 1:5 and 1:10 Vs:HA hydrogels increased during that period. This signal increase was consistent with an observed contraction of the hydrogels that likely resulted in higher concentrations of 19F contrast agent. Agitation of the 1:5 and 1:10 Vs:HA hydrogels, which was used to promote diffusion, resulted in a lower intensity of fluorine compared to non-agitated hydrogels after 1 week, but no further decrease was observed over the subsequent 2 months.

In Vitro and In Vivo Survival of GRPs in Fluorine-Labeled Hydrogels

A comparison of control ($p = 0.19$) with fluorine-labeled hydrogels with increasing ratios of Vs to HA (1:50, 1:10, 1:5) at day 1 revealed a progressively amplified BLI signal with 1.2-fold ($p = 0.19$), 1.4-fold ($p < 0.05$), and 1.8-fold increases on day 1 ($p < 0.05$), respectively. At later time points, there was a significant drop in signal, with no difference between hydrogel formulations until day 21 (Fig. 4). Subsequently, GRPs started growing in all hydrogels as spheres with a concurrent significant increase of signal in all hydrogels at day 28. Notably, fluorine seem to have had a positive effect on cell survival, as the BLI signal was directly correlated with the concentration of fluorine nanoemulsion, by factors of 1.4 ($p = 0.056$), 1.55 ($p < 0.05$), and 1.7 ($p < 0.05$) times for 1:50, 1:10, and 1:5 Vs:HA, respectively, compared to unlabeled hydrogels at day 28. Although the *in vivo* experiment included a limited sample, which precluded a statistical analysis to be performed, we demonstrated that the *in vivo* experiment seems to corroborate *in vitro* data (Fig. 5).

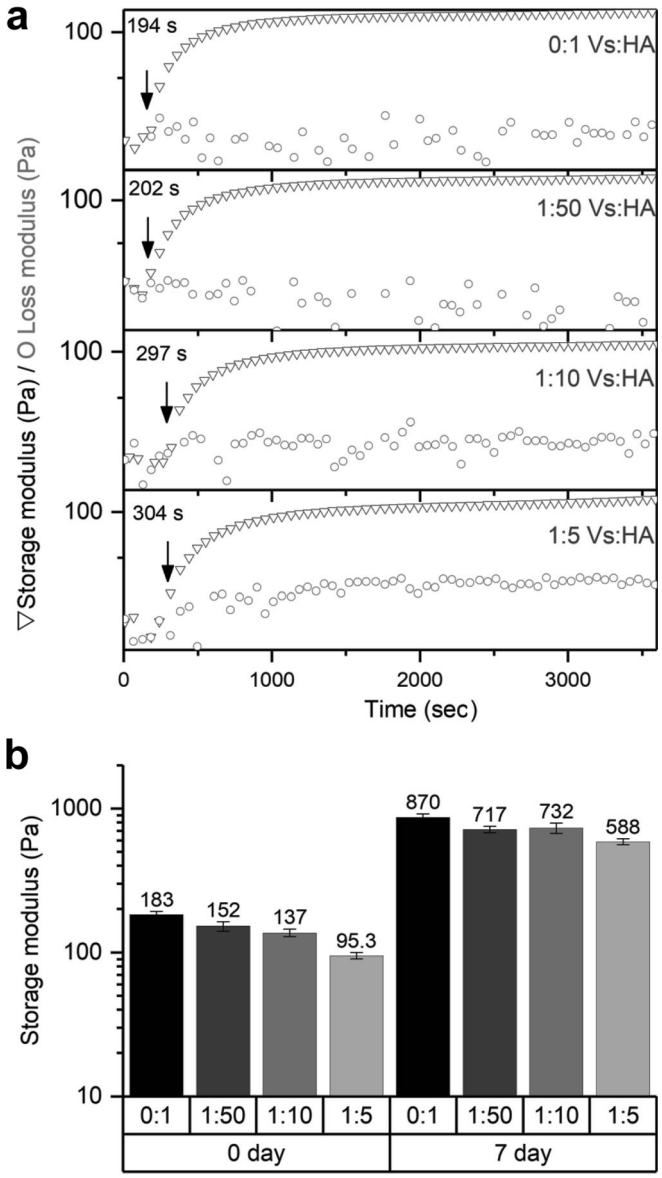

Fig. 1. Evolution of the storage modulus as a function of time. **a** Increasing concentrations of fluorine gradually elongated the gelation time from 194 s for controls to 304 s for 1:5 Vs:HA hydrogels, while **b** their elastic properties slightly decreased, from 183 pa for the controls to 95.3 pa for 1:5 Vs:HA hydrogels at day 0, and from 870 pa for the controls to 588 pa for 1:5 Vs:HA hydrogels on day 7.

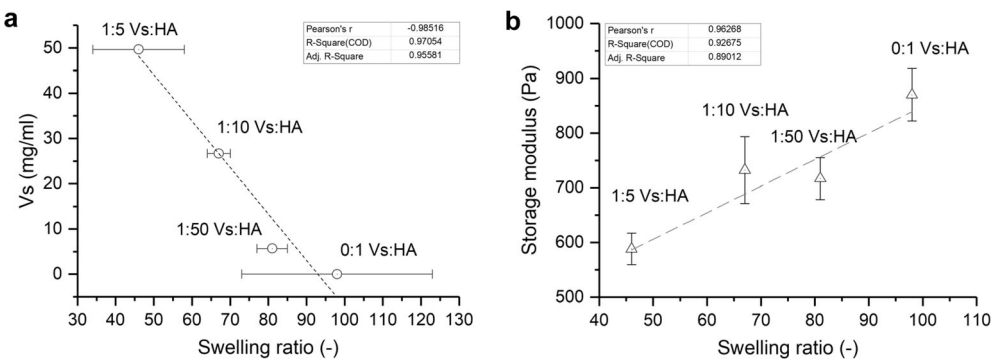

Fig. 2. **a** The swelling dependence of the perfluorocarbon nanoemulsion and **b** the relationship between the storage modulus and the swelling ratio.

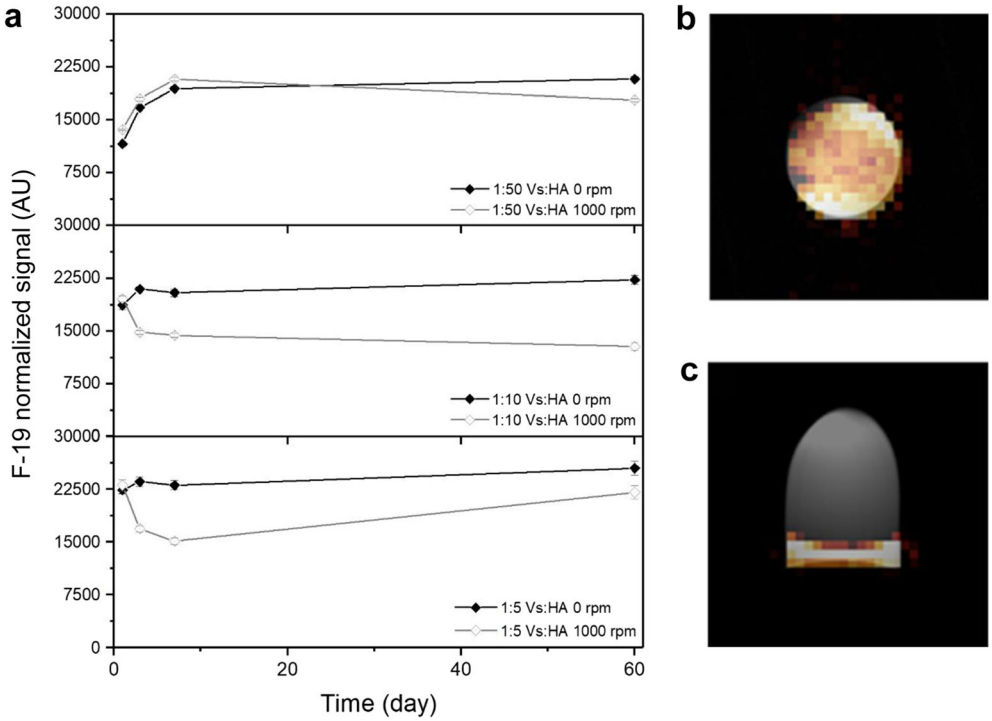

Fig. 3. **a** Normalized 19F signal as a function of time at diffusion-forced (agitation) and stationary conditions. Diffusion of the fluorine nanoemulsion from hydrogels was negligible during long-term observation at 0 rpm and 1000 rpm. **b** Cross- and **c** perpendicular MR images of a 1:10 Vs:HA hydrogel at 1 day. The 19F MR image was overlaid on the 1H MR image.

Discussion

We demonstrated the long-term stability of fluorine-labeled HA hydrogels for at least 2 months for both stationary and agitated conditions. It was previously shown that agitation did not accelerate the diffusion of blue dextran from the gel, and that diffusion was induced only after digestion [13]. It was not obvious that this could be achieved, as fluorine is volatile and disappears after the death of fluorine-labeled cells [25]. The stability of labeling over a time period of at least 2 months is appealing for long-term tracking of injected HA-based hydrogels *in vivo* using 19F MRI. With this result, and in the context of future applications, any reduction of fluorine signal should be interpreted as remodeling of the hyaluronan-based scaffold through the

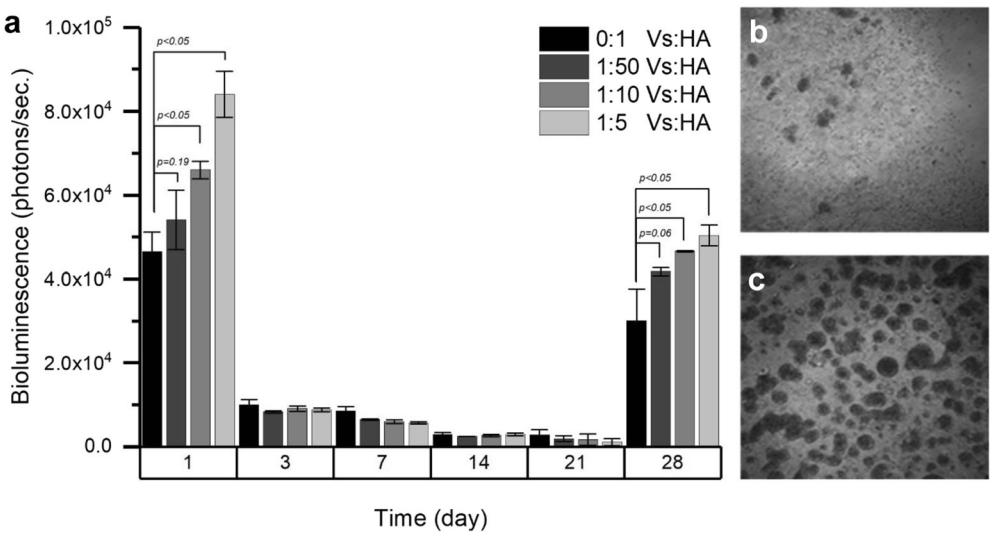

Fig. 4. **a** Viability of GRPs embedded into V-sense hydrogels over time, as assessed by BLI. The 19F emulsion increased cell survival inside the hyaluronan-based hydrogels. The reappearance of the BLI signal was reported for all Vs:HA configurations after 21 days of experiments. Representative light microscopic images of GRPs embedded in a 1:50 Vs:HA hydrogel at **b** day 7 and **c** day 28 reveal that GRPs revived and initiated formation of spheres. A two-sample *t* test was performed to calculate the statistical significance of the difference between controls and fluorine-based hydrogels.

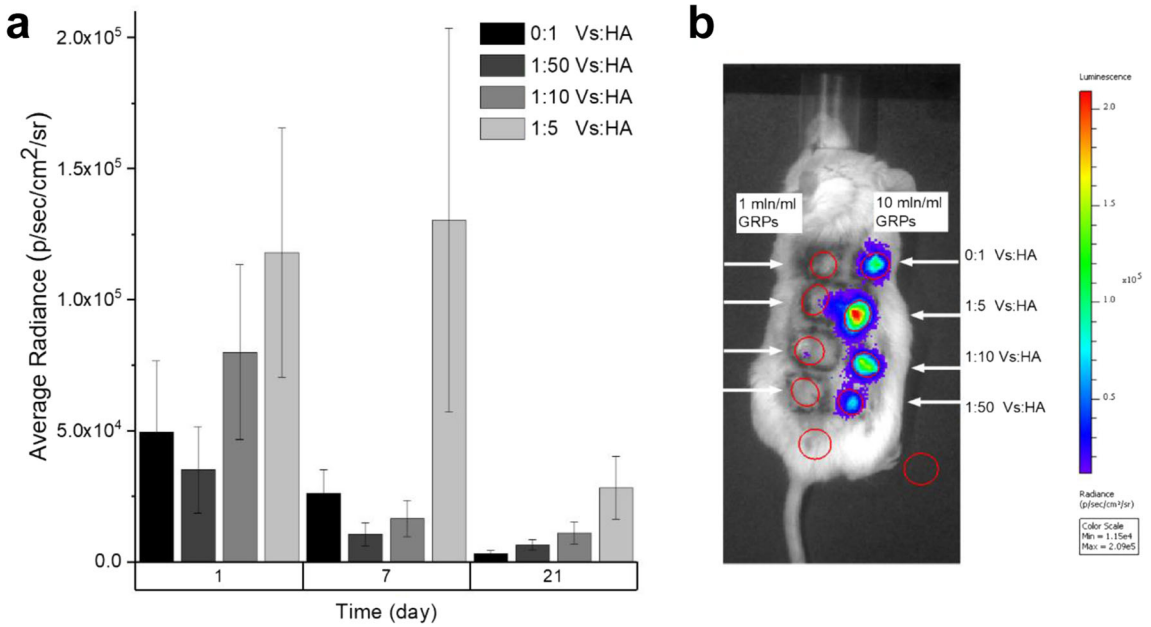

Fig. 5. **a** Vs:HA hydrogels were injected s.c. into immunodeficient mice and the viability of 1×10^6 GRPs/ml was recorded at 1, 7, and 21 days. Similar to the *in vitro* observations, the addition of Vs to the hyaluronan improved cell survival. **b** *In vivo* BLI of rag2$^{-/-}$ mice immediately after hydrogel injection. Red circles below the ROIs—backgrounds.

process of digestion, rather than spontaneous fluorine release from intact hydrogels [25, 26].

The rheological assessment revealed that the supplementation of hydrogels with a fluorine nanoemulsion decreased the G′ at day 1 and day 7 proportional to the lowering of the concentration of the cross-linkable partners, HA, and PEGDA (Table 1). Since the elastic properties of hydrogels depend on the network density inside the hydrogel [14], this process is highly reproducible, allowing for tuning hydrogel properties to achieve the desired storage modulus [27]. Both fluorine-labeled and non-labeled hydrogels become stiffer after cross-linking, as expressed by the increase in the storage modulus over a couple of days. This phenomenon is characteristic of thiol-reactive cross-linkers, as HA and PEGDA pair where bi-functional formation of the network occurs [14]. The interaction between HA-PEGDA has a short time scale (minutes) and dominates in the initial stage of hydrogel formation. Simultaneously, a longer interaction time scale (hours) between free thiols produces disulfide bonds primarily between modified hyaluronan chains. The introduction of a fluorine nanoemulsion to the HA-based hydrogels seems to have no bearing over the mechanism of network formation, and longer gelation seems to change elasticity due to volumetric replacement of HA by Vs. Nevertheless, this problem of gelation time may be an advantage when a hydrogel is to be injected using long catheters.

The *in vitro* cell survival assay revealed no detrimental effect, but rather, a pro-survival effect of fluorine nanoemulsion on GRP cell viability. The high mortality of the cells typically observed after transplantation may be due to an osmotic and oncotic turbulence during cell transplantation [28]. The tight network of a hyaluronan-based hydrogel results in cell separation with anoikis [25]. The introduction of a fluorine nanoemulsion in a hydrogel might modulate cell death and re-growth within hyaluronan-based hydrogels by lowering network density and cross-linking partners' concentration (HA and PEGDA), or by water exclusion. The nanoemulsion may also result in lowering osmotic turbulence driven by high potency to water binding by HA, which is expressed by a lower swelling ratio. The positive effect of fluorine on cell proliferation *in vitro* was pronounced when the bioluminescence signal was relatively high at the early time points and when it increased again at day 28, likely due to GRP cell proliferation. While the sample size in the *in vivo* experiment was insufficient, the preliminary results seem to be in good accordance with the *in vitro* experiments, and further experiments are needed to unequivocally confirm this in an *in vivo* setting.

The study also has some limitations. The observation time scale for cell survival experiments both *in vitro* and *in vivo* is relatively short. It provides convincing data indicating the utility of fluorine-labeled hydrogels; however, from the perspective of GRP-based therapy, a longer assessment of cell proliferation would be beneficial. The improvement of GRP survival in fluorine-labeled hydrogels might also be related to the changes in rheological properties and not to the presence of the fluorine nanoemulsion itself, but examining this would require additional studies.

Conclusions

Labeling of HA-based hydrogels with a fluorine nanoemulsion resulted in the modest altering of its

biomechanical properties, but the gelation remained robust. The long-term stability of hydrogel labeling provides the rationale for longitudinal studies, without a negative impact on GRP viability. Overall, the labeling of HA-based hydrogels with fluorine nanoemulsion may be a promising strategy with which to monitor the distribution of GRP-embedded scaffolds non-invasively using clinically applicable MRI.

Funding Information. This work was supported by R01 EB023647, R56 NS098520, MSCRFD-3899, MSCRFII=2829, R01NS091110, R01NS091100, and R21NS106436. MP was supported by the KNOW program of Jagiellonian University, Cracow, Poland.

Compliance with Ethical Standards. The study was approved by our Institutional Animal Care and Use Committee at the Johns Hopkins University.

Conflict of Interest

The authors declare that they have no conflict of interest.

References

1. Hess DC, Wechsler LR, Clark WM, Savitz SI, Ford GA, Chiu D, Yavagal DR, Uchino K, Liebeskind DS, Auchus AP, Sen S, Sila CA, Vest JD, Mays RW (2017) Safety and efficacy of multipotent adult progenitor cells in acute ischaemic stroke (masters): a randomised, double-blind, placebo-controlled, phase 2 trial. Lancet Neurol 16:360–368
2. Anderson KD, Guest JD, Dietrich WD, Bartlett Bunge M, Curiel R, Dididze M, Green BA, Khan A, Pearse DD, Saraf-Lavi E, Widerström-Noga E, Wood P, Levi AD (2017) Safety of autologous human Schwann cell transplantation in subacute thoracic spinal cord injury. J Nneurotrauma 34:2950–2963
3. Gupta N, Henry RG, Strober J, Kang SM, Lim DA, Bucci M, Caverzasi E, Gaetano L, Mandelli ML, Ryan T, Perry R, Farrell J, Jeremy RJ, Ulman M, Huhn SL, Barkovich AJ, Rowitch DH (2012) Neural stem cell engraftment and myelination in the human brain. Sci Transl Med 4:155ra137
4. Oliveira JM, Carvalho L, Silva-Correia J, Vieira S, Majchrzak M, Lukomska B, Stanaszek L, Strymecka P, Malysz-Cymborska I, Golubczyk D, Kalkowski L, Reis RL, Janowski M, Walczak P (2018) Hydrogel-based scaffolds to support intrathecal stem cell transplantation as a gateway to the spinal cord: clinical needs, biomaterials, and imaging technologies. NPJ Regen Med 3:8
5. Windrem MS, Schanz SJ, Guo M, Tian GF, Washco V, Stanwood N, Rasband M, Roy NS, Nedergaard M, Havton LA, Wang S, Goldman SA (2008) Neonatal chimerization with human glial progenitor cells can both remyelinate and rescue the otherwise lethally hypomyelinated shiverer mouse. Cell Stem Cell 2:553–565.
6. Walczak P, All AH, Rumpal N, Gorelik M, Kim H, Maybhate A, Agrawal G, Campanelli JT, Gilad AA, Kerr DA, Bulte JWM (2011) Human glial-restricted progenitors survive, proliferate, and preserve electrophysiological function in rats with focal inflammatory spinal cord demyelination. Glia 59:499–510
7. Lyczek A, Arnold A, Zhang J, Campanelli JT, Janowski M, Bulte JWM, Walczak P (2017) Transplanted human glial-restricted progenitors can rescue the survival of dysmyelinated mice independent of the production of mature, compact myelin. Exp Neurol 291:74–86
8. Glass JD, Hertzberg VS, Boulis NM, Riley J, Federici T, Polak M, Bordeau J, Fournier C, Johe K, Hazel T, Cudkowicz M, Atassi N, Borges LF, Rutkove SB, Duell J, Patil PG, Goutman SA, Feldman EL (2016) Transplantation of spinal cord-derived neural stem cells for als: analysis of phase 1 and 2 trials. Neurology 87:392–400
9. Jablonska A, Shea DJ, Cao S, Bulte JW, Janowski M, Konstantopoulos K, Walczak P (2017) Overexpression of vla-4 in glial-restricted precursors enhances their endothelial docking and induces diapedesis in a mouse stroke model. J Cereb Blood Flow Metab. https://doi.org/10.1177/0271678X17703888
10. Guzman R, Janowski M, Walczak P (2018) Intra-arterial delivery of cell therapies for stroke. Stroke 49:1075–1082
11. Slevin M, Kumar S, Gaffney J (2002) Angiogenic oligosaccharides of hyaluronan induce multiple signaling pathways affecting vascular endothelial cell mitogenic and wound healing responses. J Biol Chem 277:41046–41059
12. Shu XZ, Liu Y, Palumbo F, Prestwich GD (2003) Disulfide-crosslinked hyaluronan-gelatin hydrogel films: a covalent mimic of the extracellular matrix for in vitro cell growth. Biomaterials 24:3825–3834
13. Shu XZ, Liu Y, Luo Y, Roberts MC, Prestwich GD (2002) Disulfide cross-linked hyaluronan hydrogels. Biomacromolecules 3:1304–1311
14. Ghosh K, Shu XZ, Mou R, Lombardi J, Prestwich GD, Rafailovich MH, Clark RAF (2005) Rheological characterization of in situ cross-linkable hyaluronan hydrogels. Biomacromolecules 6:2857–2865
15. Prestwich GD (2011) Hyaluronic acid-based clinical biomaterials derived for cell and molecule delivery in regenerative medicine. J Control Release 155:193–199
16. Liang Y, Walczak P, Bulte JW (2013) The survival of engrafted neural stem cells within hyaluronic acid hydrogels. Biomaterials 34:5521–5529
17. Laurén P, Lou YR, Raki M, Urtti A, Bergström K, Yliperttula M (2014) Technetium-99m-labeled nanofibrillar cellulose hydrogel for in vivo drug release. Eur J Pharm Sci 65:79–88
18. Kim H, Shin K, Park OK, Choi D, Kim HD, Baik S, Lee SH, Kwon SH, Yarema KJ, Hong J, Hyeon T, Hwang NS (2018) General and facile coating of single cells via mild reduction. J Am Chem Soc 140:1199–1202
19. Hosoya H, Dobroff AS, Driessen WH, Cristini V, Brinker LM, Staquicini FI, Cardó-Vila M, D'Angelo S, Ferrara F, Proneth B, Lin YS, Dunphy DR, Dogra P, Melancon MP, Stafford RJ, Miyazono K, Gelovani JG, Kataoka K, Brinker CJ, Sidman RL, Arap W, Pasqualini R (2016) Integrated nanotechnology platform for tumor-targeted multimodal imaging and therapeutic cargo release. Proc Natl Acad Sci USA 113:1877–1882
20. Liang Y, Bar-Shir A, Song X, Gilad AA, Walczak P, Bulte JWM (2015) Label-free imaging of gelatin-containing hydrogel scaffolds. Biomaterials 42:144–150
21. Bulte JW (2005) Hot spot MRI emerges from the background. Nat Biotechnol 23:945–946
22. Ahrens ET, Helfer BM, O'Hanlon CF, Schirda C (2014) Clinical cell therapy imaging using a perfluorocarbon tracer and fluorine-19 MRI. Magn Reson Med 72:1696–1701
23. Muhammad G, Xu J, Bulte JWM, Jablonska A, Walczak P, Janowski M (2017) Transplanted adipose-derived stem cells can be short-lived yet accelerate healing of acid-burn skin wounds: a multimodal imaging study. Sci Report 7:4644.
24. Rubinstein M, Colby R, Dobrynin AV, Joanny JF (1996) Elastic modulus and equilibrium swelling of polyelectrolyte gels. Macromolecules 29:398–406
25. Bonnans C, Chou J, Werb Z (2014) Remodelling the extracellular matrix in development and disease. Nat Rev Mol Cell Biol 15:786–801
26. Carey LE, Dearth CL, Johnson SA, Londono R, Medberry CJ, Daly KA, Badylak SF (2014) In vivo degradation of 14c-labeled porcine dermis biologic scaffold. Biomaterials 35:8297–8304
27. Shu XZ, Liu Y, Palumbo FS (2004) In situ crosslinkable hyaluronan hydrogels for tissue engineering. Biomaterials 25:1339–1348
28. Mohand-Kaci F, Assoul N, Martelly I, Allaire E, Zidi M (2013) Optimized hyaluronic acid-hydrogel design and culture conditions for preservation of mesenchymal stem cell properties. Tissue Eng Part C Methods 19:288–298